Iranian Journal of Science & Technology, Transaction B, Engineering, Vol. 32, No. B1, pp 39-51
Printed in The Islamic Republic of Iran, 2008

EFFECT OF ASPECT RATIO AND FILLING RATIO ON THERMAL PERFORMANCE OF AN INCLINED TWO-PHASE CLOSED THERMOSYPHON*

M. R. SARMASTI EMAMI[1], S. H. NOIE[2**] AND M. KHOSHNOODI[1]

[1]Dept. of Chem. Eng., University of Sistan and Baluchestan, Zahedan, I. R. of Iran
[2]Dept. of Chem. Eng., Faculty of Engineering, Ferdowsi University of Mashhad, Mashhad, P.O. Box. 9177948944-1111, I. R. of Iran, Email: noie@um.ac.ir

Abstract– In this paper the effect of the aspect ratio and filling ratio on the thermal performance of an inclined two-phase closed thermosyphon under normal operating conditions has been investigated experimentally. The experiments were carried out for filling a ratio range of 20%≤F.R≤60% and aspect ratios of 15, 20, and 30 for an inclination angle range of 15°≤Φ≤90°. The thermosyphon was manufactured using a copper tube with an inside and outside diameter of 14 and 16 mm respectively, and a 1000 mm length. Distilled water was used as the working fluid. The heat transfer rate, temperature distribution, and condensation heat transfer coefficient of the inclined two-phase closed thermosyphon were measured. The results showed that the maximum thermal performance of the thermosyphon occurred at 60° for all three aspect ratios and several filling ratios. The thermal performance of the inclined thermosyphon with an inclination angle of 60° was better for a filling ratio of 45%. It was also found that a higher condensation heat transfer coefficient for all three aspect ratios took place between 30 and 45 degrees.

Keywords– Inclined two-phase closed thermosyphon, inclination angle, filling ratio, aspect ratio

1. INTRODUCTION

Grover [1] (Los Alamos Laboratory, USA) introduced the term heat pipe in 1964. The two-phase closed thermosyphon used in this study is essentially a gravity-assisted wickless heat pipe, which is very efficient for the transport of heat with a small temperature difference via the phase change of the working fluid. It consists of an evacuated-closed tube filled with a certain amount of a suitable pure working fluid. The simple design, operation principle, and the high heat transport capabilities of two-phase closed thermosyphons are the primary reasons for their wide use in many industrial and energy applications. Since there is no wick material, the thermosyphon is simpler in construction, smaller in thermal resistance, and wider in its operating limits than the wicked heat pipe.

In practice, the effective thermal conductivity of a thermosyphon exceeds that of copper by a factor of 200–500 [2]. This is achieved by the evaporation of the working fluid (A) in the evaporator section (B), condensing in the condenser section (C), and the return of the condensate (D), as shown in Fig. 1.

The operating characteristics of vertical two-phase closed thermosyphons have been investigated extensively in recent years [3-9]. Little information is available for the thermal performance of inclined two-phase closed thermosyphons. Negishi and Sawada [10] made an experimental study on the heat transfer performance of an inclined two-phase closed thermosyphon. They used water and ethanol as working fluids. The highest heat transfer rate was obtained when the filling ratio (ratio of volume of

*Received by the editors September 5, 2005; final revised form February 21, 2007.
**Corresponding author

working fluid to volume of evaporator section) was between 25% and 60% for water and between 40% and 75% for ethanol. The inclination angle was between 20° and 40° for water, and more than 5° for ethanol.

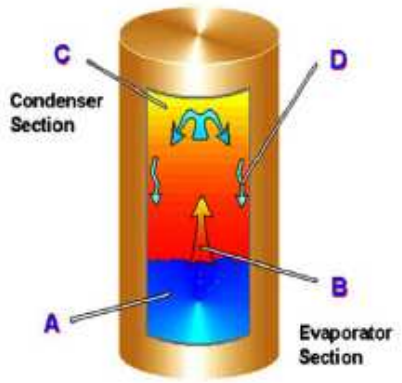

Fig. 1. Schematic diagram of a two-phased closed thermosyphon

Wangnippanto [11] studied the effect of the inclination angle on the heat transfer rate of a thermosyphon using a copper-water thermosyphon having an inside diameter of 20 mm and a length of 810 mm. He concluded that the angle at which the highest heat transfer rate occurred was 22.5° with a filling ratio of 30%. Zuo and Gunnerson [12] studied the heat transfer of an inclined two-phase closed thermosyphon. They showed that the minimum amount of working fluid remains almost constant from 20º to 90º, with respect to the horizontal axis, and then significantly increase by deceasing the inclination angle. They also found that the highest flooding limit is at an inclination angle ranging from 45º to 60º.

Terdtoon *et al*. [13] investigated the effect of the aspect ratio (ratio of evaporator section length to inside diameter of pipe) and Bond number on the heat transfer characteristics of an inclined two-phase closed thermosyphon experimentally. They found that the optimum inclination angle (from horizontal axis) for water is between 70° and 80° from a horizontal axis. They also found that the value of Q_i/Q_{90} gradually decreases in the range of $L_e/D_i<10$, but it is nearly constant at $L_e/ D_i >10$.

Booddachan *et al*. [14], studied the effect of inclination angles, aspect ratios and Bond number on the heat transfer performance of a two-phase closed HDPE (high density polyethylene) thermosyphon working under normal operation conditions. The HPDE thermosyphon used in the experiment had inside diameters of 15, 20 and 25 mm. The evaporator, adiabatic and condenser sections were all of the same length at all aspect ratios. R113 and R11 were used as working fluids with a filling ratio of 50%. The inclination angles were 5, 10, to 90 degrees with the horizontal axis. The aspect ratios were 5, 10, 20 and 30. The results showed the inclination angle with maximum heat transfer performance ranged from 60-70 degrees. Payakaruk *et al*. [15] investigated the heat transfer characteristics of copper thermosyphons with inner diameters of 7.5, 11.1 and 25.4. Water, ethanol, R-22, R-123, and R-134a were used as working fluids, and it was found that the optimum inclination angle for water is between 40° and 70°.

Wang and Ma [16] studied condensation heat transfer inside vertical and inclined thermosyphons. They found that the inclination angle has a notable influence on the condensation coefficient, and the optimum inclination angle varies with liquid filling from 20- 50 degrees.

Hussein *et al*. [17] developed the Wang and Ma correlation for laminar-film condensation heat transfer inside inclined wickless heat pipes flat-plate solar collector. They found that Le/ D_i and the inclination angle have a significant effect on the condensation heat transfer inside inclined wickless heat pipes.

Shiraishi *et al*. [18] has experimentally investigated the critical heat transfer rate in an inclined thermosyphon by taking account of the aspect ratio, filling ratio, working fluid property, and operating pressure. They found that $Q_{c,i}/Q_{c,90}$ can be correlated well with the modified Kutateladze number with an accuracy of ±10%. Also, the density ratio of working fluid ($\rho_v/\ \rho_l$) correlated well with $Q_{c,i}/Q_{c,90}$, with an accuracy range of ±15%.

Due to differences in operating conditions, the diverse values of the optimum inclination angle, and the lack of research on the effect of aspect ratio (especially for $L_e/\ D_i > 10$) and filling ratio on the inclined situation of a two-phase closed thermosyphon, the effect of filling ratio and aspect ratio on the thermal performance of an inclined two-phase closed thermosyphon has been investigated experimentally in this research.

2. EXPERIMENTAL SETUP

In order to study the thermal performance of an inclined two-phase closed thermosyphon, a specific experimental setup was designed and constructed. The schematic of the experimental test rig is shown in Fig. 2, the main parts of which are:

Thermosyphon (1)
Water Jacket (2)
Liquid Tank (3)
Rotameter (4)
Electric Heater (5)
Thermocouples (6)
Data Logger (7)
Personal Computer (8)

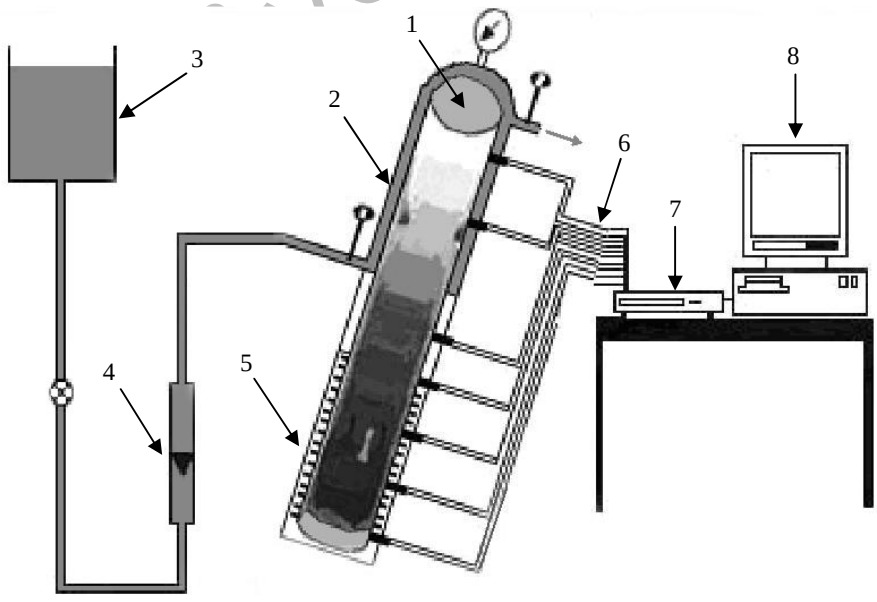

Fig. 2. The experimental test rig

The thermosyphon was 1000 mm in length with an outside diameter of 16 mm, and an inside diameter of 14 copper tubes. The length of the condenser section was 410 mm, but the length of the

adiabatic section and evaporator section are variable depending on the aspect ratio. A summary of the design specifications for the thermosyphon is given in Table 1.

Table 1. Design summary of the thermosyphon

No.	D_i(mm)	L_e(mm)	L_a(mm)	L_e/D_i
1	14	210	380	15
2	14	280	310	20
3	14	410	180	30

Water has good thermophysical properties such as the heat of vaporization and can be used in a wide range of temperatures (303-473 K) [19]. Therefore, water was used as a working fluid in our experiments. A 410 mm long water jacket surrounds the condenser section, and cooling water flows through the annular passage of the jacket. A constant head tank was placed two meters above the head of the thermosyphon and connected to the cooling section by a plastic pipe. The electric heater of the evaporator section was made of a Nickel-Chrome wire with a nominal power of 1000 W. The electric heater was covered by an electrically insulated tape and rock wool insulation of 32 mm thick. Also, the other sections of the thermosyphon were covered by rock wool as well, to reduce the heat loss by radiation and convection to the surroundings.

3. EXPERIMENTAL PROCEDURE

The experiment was performed as follows:

Before charging the thermosyphon, the tube was cleaned thoroughly to remove any grease or oil from the inner surface. After charging the tube with working fluid, we must assure the absence of non-condensable gases in the tube. This problem is very important, especially for a low temperature thermosyphon. In order to eliminate the non-condensable gas, a slightly more than exact quantity of working fluid was injected into the tube after evacuating the air. A small amount of non-condensable gas was collected at the end of the condenser after a few minutes of operation. This gas was removed again by a vacuum pump to ensure the perfect operation of the thermosyphon. All of the residual working fluid in the test tube was collected after each experimental run and its volume was measured to compare with the exact quantity of working fluid. Vacuuming was down to 0.001 mm.

Temperature distribution along the external surface of the thermosyphon was measured by seven Ni-Cr thermocouples mechanically attached to the surface of the pipe. The thermocouples were glued by a high conductive epoxy. The operating pressure was measured by a pressure transducer connected to the upper part of the thermosyphon. For temperature measurement in the condenser section, thermocouples were mounted on the water jacket, but pressed against the external surface of the inner pipe of the thermosyphon through a screw arrangement. All thermocouples were connected to a data-logger which was, in turn, connected to a computer for displaying data.

The flow rate of cooling water was measured by a rotameter. The input and output temperatures of the water jacket were measured by two digital “TESTO” thermometers. The accuracy of measurements was approximately ± 1°C for temperatures of the external surface pipe, $\pm$ 0.1°C for input and output water, ± 4% for the water flow rate, and ± 2% for the pressure measurement. A series of experiments were carried out in order to investigate the thermal performance of the inclined two-phase closed thermosyphon.

4. HEAT TRANSFER RATE

The following calculations were carried out to determine the input and output heat transfer rate of the thermosyphon. The actual heat input to the evaporator section was obtained from Eq. (1).

$$Q_{in} = VI - Q_{loss} \tag{1}$$

where Q_{loss} is the sum of heat losses from the evaporator section by radiation and free convection.

$$Q_{loss} = Q_{rad.} + Q_{conv.} \tag{2}$$

The radiation heat transfer rate was evaluated from Eq. (3)

$$Q_{rad.} = \varepsilon \sigma A_e (T_{ins.}^4 - T_{air}^4) \tag{3}$$

and free convection heat transfer was calculated from Eq. (4).

$$Q_{conv.} = h_{conv.} A_e (T_{ins.} - T_{air}) \tag{4}$$

Free convection heat transfer coefficient on a vertical and inclined cylinder was evaluated from Churchill and Chu [20]. (Eq. (5)).

$$Nu = \frac{h_{conv.} L_e}{k_{air}} = \left\{ 0.825 + \frac{0.387 Ra^{1/6}}{\left[1 + \left(\frac{0.492}{Pr} \right)^{9/16} \right]^{8/27}} \right\}^2 \tag{5}$$

where Ra (Rayleigh number) was evaluated from Eq. (6).

$$Ra = g\beta(T_{ins.} - T_{air}) L_e^3 / \alpha\nu \tag{6}$$

Incropera and De Witt [21] recommended that for $30^\circ \leq \Phi < 90^\circ$, g can be replaced by $g\sin\Phi$ and Eq. (6) is used to compute average Nusselt Number. Hence, the sum of heat loss was about 2.34%, 2.67% and 2.93% of input power to the evaporator section for aspect ratios of 15, 20 and 30 respectively.

The heat transmitted from the condenser section is equal to the rejected heat to coolant water in the jacket, and was calculated from Eq. (7).

$$Q_{out} = \dot{m} c_{p,w} (T_{o,w} - T_{i,w}) \tag{7}$$

5. HEAT TRANSFER LIMITATIONS

There are various parameters that put limitations and constraint on the steady and transient operation of a two-phase closed thermosyphon. Physical phenomena that might limit heat transport in two-phase closed thermosyphons are due to dry-out, flooding (or entrainment), and boiling. The dry-out limit is the easiest to avoid by providing a sufficient amount of working fluid into the thermosyphon at startup (F.R≥20%) [8]. Since, in this work the filling ratios are higher than 20%, only the boiling and flooding limits are examined.

Because the input heat is rather low, the boiling limit is evaluated based on a correlation proposed by Gorbis and Savchenkov [22].

$$Q_{c,90} = Ku\left\{h_{fg}\rho_v^{0.5}\left[\sigma g(\rho_l - \rho_v)\right]^{0.25}\right\} \quad (8)$$

where

$$Ku = 0.0093(A.R)^{-1.1}\left(\frac{D_i}{L_c}\right)^{-0.88}(F.R)^{-0.74}(1+0.03Bo)^2 \qquad 2<Bo<60 \quad (9)$$

The flooding limit is evaluated based on a correlation proposed by Faghri [19].

$$Q_{c,90} = Kh_{fg}A_{cross}\left[g\sigma(\rho_l - \rho_v)^{1/4}\right]\times\left[\rho_v^{-1/4} + \rho_l^{-1/4}\right]^{-2} \quad (10)$$

where

$$K = \left(\frac{\rho_l}{\rho_v}\right)^{0.14}\tanh^2(Bo)^{1/4} \quad (11)$$

The above correlations are used for the vertical situation of a thermosyphon. For the inclined thermosyphon the following correlation is used for the calculation of the both boiling limit and the flooding limit, presented by Shiraishi *et al.* [18].

$$(12)\quad Q_{c,i}/Q_{c,90} = 1 + 0.13\left\{\left[\frac{(\rho_v/\rho_l)^{1/2} + 0.05}{(\rho_v/\rho_l) + 0.05}\right]^2 - 1\right\}$$

6. CONDENSATION HEAT TRANSFER COEFFICIENT

Experimental condensation heat transfer coefficient is evaluated from the following equation.

$$h_c = \frac{Q_{out}}{A_c(T_v - T_{c,m})} \quad (13)$$

The condenser temperature, $T_{c,m}$, is calculated by the arithmetic mean of the surface temperatures of the condenser section. T_v is vapor temperature that, in this research, was considered to be equal to adiabatic temperature as discussed by [23 and 24].

7. RESULTS AND DISCUSSION

In this work the operating parameters studied were:

A: Controlled parameters:

Working fluid	Distilled water
Condenser length	41 cm
Material of tube	Copper
Input heat to evaporator section	200 W

B: Variable parameters:

Filling ratio	20%≤ F.R ≤60%
Aspect ratio	15, 20, 30
Inclination angle	15, 30, 45, 60, 75, 90

A series of experiments were carried out to find the effect of variable parameters on the thermal performance of the inclined two-phase closed thermosyphon. The heat transfer rate for inclined positions

(Q_i) is normalized by dividing it to the value of the vertical position (Q_{90}) in order to clarify the effect of the inclination angle. In the following sections, after calculation of the heat transfer limitations, the effects of the aspect ratio and filling ratio on the heat transfer rate of an inclined two-phase closed thermosyphon are considered. The temperature distribution along the inclined thermosyphon and condensation heat transfer coefficient are then examined.

a) Calculation of heat transfer limitations

The values of $Q_{c,i}/Q_{c,90}$ are calculated using Eq. (12). Due to the low operating temperature of an inclined two-phase closed thermosyphon, the value of $Q_{c,i}/Q_{c,90}$ is varied in a range of 1.032 to 1.042, which is very low. Therefore, the flooding and boiling limits are calculated for various filling ratios and aspect ratios using the Eqs. (8) and (10) at vertical situation. The results are listed in Tables 2, 3 and 4.

Table 2. Heat transfer limits for A.R=15

Filling ratio / Limit	20%	35%	45%
Flooding	1054 W	1054 W	1054 W
Boiling	868 W	563 W	492 W

Table 3. Heat transfer limits for A.R=20

Filling ratio / Limit	25%	40%	45%
Flooding	1080 W	1080 W	1080 W
Boiling	616 W	421 W	368 W

Table 4. Heat transfer limits for A.R=30

Filling ratio / Limit	30%	45%	60%
Flooding	1137 W	1137 W	1137 W
Boiling	355 W	263 W	212 W

As can be seen from the tables above, the values for boiling limits are lower than those for flooding. Therefore, the effect of the aspect ratio on boiling limit was only investigated. Table 5 shows the boiling limit for aspect ratios 15, 20 and 30.

Table 5. Effect of aspect ratio on boiling limit for F.R=45%

Aspect ratio / Limit	15	20	30
Boiling	492 W	368 W	263W

As shown in Table 5 as the boiling limit decreased, the aspect ratio increased. The lower limit between the two constraints defines the maximum heat transport limitation of the thermosyphon. Since the input heat (200W) is lower than all heat transfer limits, the thermosyphon operates without any problem.

b) Effect of filling ratio

In order to find out the effect of the filling ratio on the heat transfer rate of the inclined two-phase closed thermosyphon, the experimental results are plotted in Figs. 3 and 4. Figure 3 shows the variation of Q_i/Q_{90} against the inclination angle for three filling ratios of 20%, 35%, and 45% for aspect ratio 15.

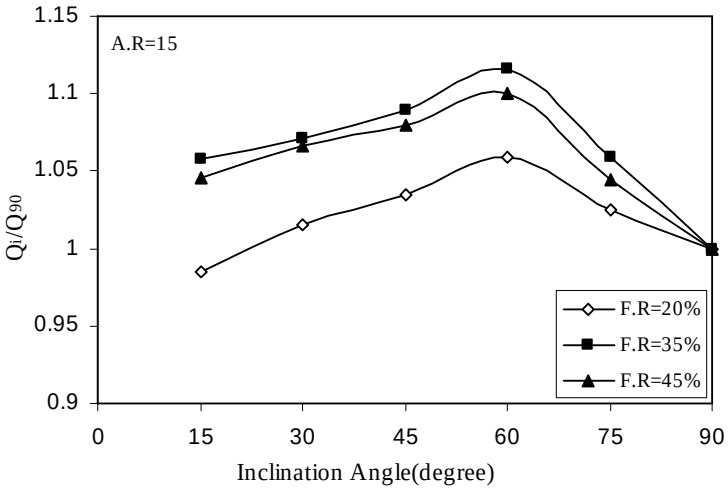

Fig. 3. Effects of filling ratio and the inclination angle on the Q_i/Q_{90} for A.R=15

From this figure it can be seen that:
-The values of Q_i/Q_{90} for a filling ratio of 35% are higher than those for other filling ratios.
-Maximum heat transfer rate (Q_i/Q_{90}) for all three filling ratios takes place at Φ=60°.

Figure 4 shows the variation of Q_i/Q_{90} with the inclination angle for three filling ratios of 30%, 45%, and 60% for aspect ratio 30.

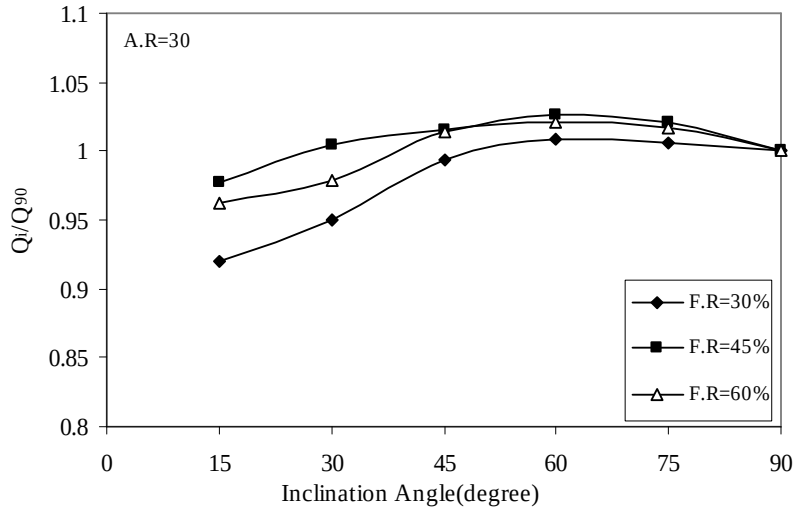

Fig. 4. Effects of filling ratio and the inclination angle on the Q_i/Q_{90} for A.R=30

As shown in Fig. 4:
-The values of Q_i/Q_{90} for a filling ratio of 45% are higher than those for other filling ratios.
-Maximum heat transfer rate (Q_i/Q_{90}) for all three filling ratios again take place at Φ=60°.
Therefore, it can be concluded from Figs. 3 and 4 that:

-Higher value of Q_i/Q_{90} for each aspect ratio takes place at different filling ratios. For example, for an aspect ratio of 15, the higher Q_i/Q_{90} occurs when the filling ratio is 35%, and for an aspect ratio of 30, the filling ratio for a higher value of Q_i/Q_{90} is 45%.
-Maximum heat transfer rate (Q_i/Q_{90}) for all filling ratios and aspect ratios takes place at Φ=60°.
-On the whole, the effect of a filling ratio on the heat transfer rate is higher when the aspect ratio is lower.

c) Effect of aspect ratio

In this section, the effects of aspect ratio on the heat transfer rate of an inclined two-phase closed thermosyphon are examined. The aspect ratio varies with changes in the length of the evaporator section, while the diameter of the thermosyphon is constant. In spite of the constant input heat to the evaporator section, since the length of the evaporator is changed, the heat losses from thermosyphon are varied. Therefore, the results are shown in the form of an effectiveness factor (Q_{out}/Q_{in}) for each inclination angle. Figure 5 shows the variation of Q_{out}/Q_{in} versus the inclination angle for all three aspect ratios and for F.R=45%.

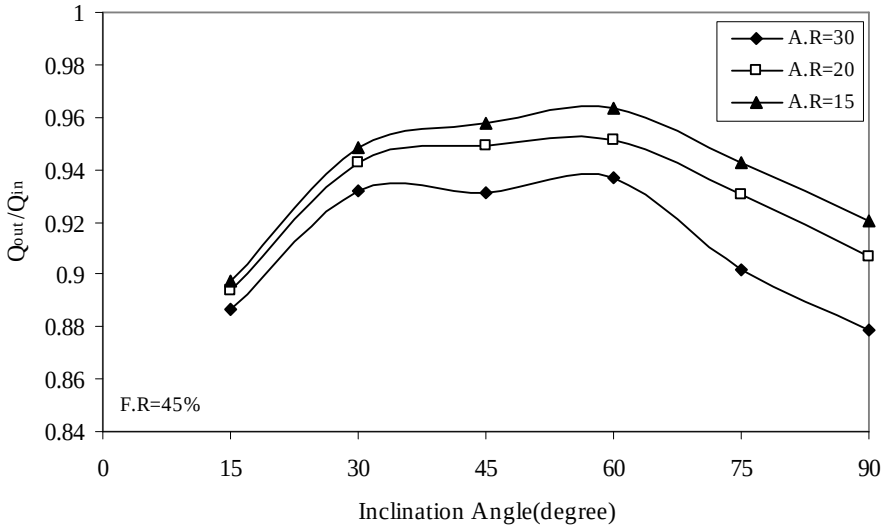

Fig. 5. Variation of Q_{out}/Q_{in} with the inclination angle for all three aspect ratios and F.R=45%

As can be seen from Fig. 5:
-The value of the effectiveness (Q_{out}/Q_{in}) factor is increased as the aspect ratio is decreased.
-The maximum heat transfer takes place at Φ=60° for all three aspect ratios.

d) Temperature distribution along the outside wall of the inclined thermosyphon (Φ=60°)

As was found in previous sections, the maximum heat transfer rate of the inclined two-phase closed thermosyphon occurred at an inclination angle of 60°. Therefore, we examined the temperature distribution along the thermosyphon for this situation.

In order to observe the temperature distribution over the entire length of the inclined thermosyphon, the temperatures at four points on the evaporator section, one point on the adiabatic section, and two points on the condenser section, are simultaneously monitored, as shown in Fig. 2.

Figure 6 shows the variation of the temperature along the inclined thermosyphon (Φ=60°) for an aspect ratio of 30 and three different filling ratios (30%, 45% and 60%). As shown in this figure, the temperature difference between the evaporator section and the condenser section for a filling ratio of 45% is lower than the other filling ratios. Therefore, the thermal performance of the inclined thermosyphon with an inclination angle of 60° is better for a filling ratio of 45%.

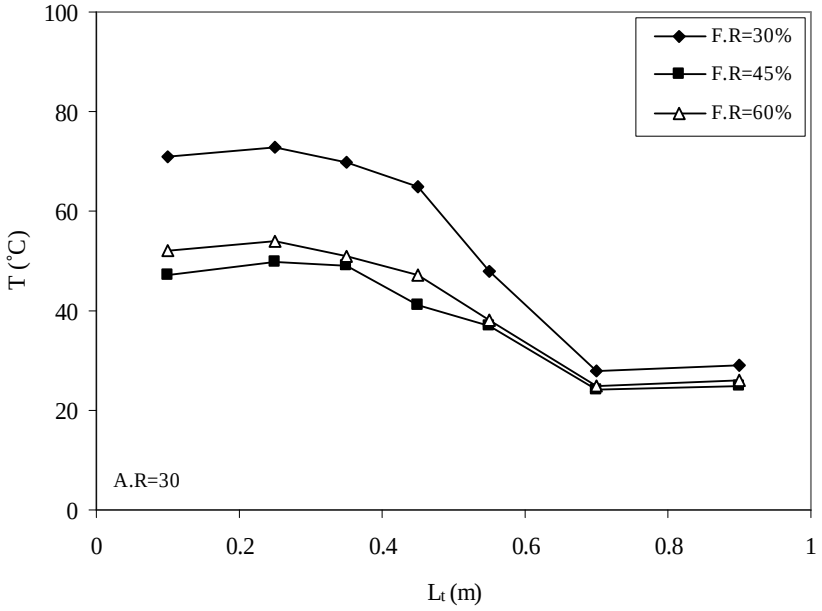

Fig. 6. Variation of the temperature along the inclined thermosyphon with Φ=60° for A.R=30

e) Heat transfer in the condenser section

Figure 7 shows the variation of the condensation heat transfer coefficient (Eq. (13)) for aspect ratios 15, 20 and 30 and the filling ratio of 45% versus the inclination angle. As shown in this figure, the maximum condensation heat transfer coefficient for all three aspect ratios occurs between 30 to 45 degrees. Furthermore, with a decreasing aspect ratio the condensation heat transfer coefficient is increased.

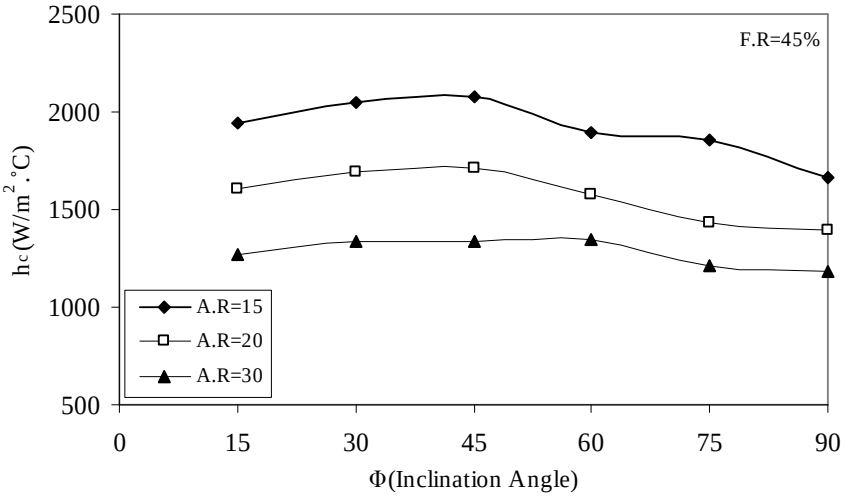

Fig. 7. Variation of h_c versus inclination angle for A.R=15, 20 and 30

8. CONCLUSION

The effect of the aspect ratio and filling ratio on the thermal performance of an inclined two-phase closed thermosyphon under normal operating conditions has been investigated experimentally. The conclusions are as follows**.**

1. The maximum heat transfer rate (Q_i/Q_{90}) for all three filling ratios and all three aspect ratios takes place at an angle of 60° with respect to the horizontal axis.
2. The thermal performance of the inclined thermosyphon with an inclination angle of 60° is better for a filling ratio of 45%.
3. The higher value of Q_i/Q_{90} for each aspect ratio takes place at different filling ratios. For example, for an aspect ratio of 15, the higher Q_i/Q_{90} occurs when the filling ratio is 35%, and also for an aspect ratio of 30, while the filling ratio for a higher value of Q_i/Q_{90} is 45%.
4. The effect of the filling ratio on the heat transfer rate is higher when the aspect ratio is lower.
5. The value of the effectiveness factor, (Q_{out}/Q_{in}) increases as the aspect ratio decreases.
6. The maximum heat transfer takes place at Φ=60° for all three aspect ratios for a filling ratio of 45%.
7. Maximum condensation heat transfer coefficient for all three aspect ratios takes place between 30 and 45 degrees, and its value is increased with the decrease of the aspect ratio.

NOMENCLATURE

A_c	condenser lateral surface (m^2)
A_e	evaporator lateral surface (m^2)
A_{cross}	cross –sectional area of pipe (m^2)
A.R	aspect ratio, ratio of evaporator section length to inside diameter of pipe (= L_e/D_i)
Bo	Bond number ($= D_i \sqrt{g(\rho_l - \rho_v)}/\sigma$)
$c_{p,w}$	specific heat of water with constant pressure (J/kg.°C)
D_i	internal diameter of pipe (m)
F.R	filling ratio, ratio of volume of working fluid to volume of evaporator section (= V_l/V_e)
g	gravitational acceleration (m/s^2)
$h_{conv.}$	convection heat transfer coefficient ($W/m^2.°C$)
h_c	condensation heat transfer coefficient ($W/m^2.°C$)
h_{fg}	latent heat of vaporization (J/kg)
I	current (A)
k_{air}	thermal conductivity of air (W/m.°C)
Ku	Kutateladze number
K	modified Kutateladze number $\{= \left(\frac{\rho_l}{\rho_v}\right)^{0.14} \tanh^2 (Bo)^{1/4}\}$
L_c	condenser length (m)
L_e	evaporator length (m)
L_t	total length of pipe (m)
$\dot{m}$	mass flow rate of water (kg/s)
Nu	Nusselt number (=$h_{conv.} L_e / k_{air}$)
Pr	Prandtl number (= υ/α)
Q_{in}	input heat into the evaporator section (W)
Q_i	heat transfer rate at inclined situation (W)
Q_{90}	heat transfer rate at vertical situation (W)
$Q_{c,i}$	heat transfer rate limits at inclined thermosyphon (W)
$Q_{c,90.}$	heat transfer rate limits at vertical thermosyphon (W)
$Q_{conv.}$	convection heat transfer rate (W)
Q_{loss}	heat loss by radiation and convection (W)

Q_{out} transmitted heat from the condenser section (W)
Q_{rad} radiation heat transfer rate (W)
Ra Rayleigh number ($= g\beta(T_{ins.} - T_{air})L_e^3 / \alpha\nu$)
T_{air} air temperature (°C)
$T_{c,m}$ average temperature of wall of condenser section (°C)
$T_{ins.}$ temperature on external surface of insulation (°C)
$T_{i,w}$ inlet water temperature of condenser (°C)
$T_{o,w}$ outlet water temperature of condenser (°C)
T_v vapor temperature (°C)
V voltage (V)
V_e evaporator volume (m^3)
V_l liquid volume (m^3)
V_t internal volume of pipe (m^3)

Greek Symbols

α thermal diffusivity of air (m^2/s) ($=k/\rho.c_p$)
β inverse of film temperature of air (K^{-1}) ($=1 / T_f$)
ν kinematic viscosity of air (m^2/s) ($=\mu/\rho$)
ρ_l density of liquid (kg/m^3)
ρ_v density of vapor (kg/m^3)
σ Stefan Boltzmann constant in Eq.(3) ($W/m^2.K^4$) and surface tension (N/m) in other Equations.
ε emissive factor of insulator
Φ inclination angle (measured against horizontal)

REFERENCES

1. Grover, G. M. (1964). Evaporation-condensation heat transfer device. US Patent, No.3229759.
2. Dunn, P. D. & Reay, D. A. (1994). *Heat Pipes*. Third Edition, Pergamon Press.
3. Lee, Y. & Mital, U. (1972). A TPCT. *Int. J. Heat Mass Transfer*, Vol. 15, pp. 1695-1707.
4. Li, H., Akbarzadeh, A. &, Johnson, A. (1991). The thermal characteristics of a closed two-phase thermosyphon at low temperature difference. *Heat Recovery Systems & CHP*, Vol. 11, No. 6, pp. 533-540.
5. Sauciuc, I., Akbarzadeh, A. & Johnson, P. (1995). Characteristics of TPCTs for medium temperature heat recovery applications. *Heat Recovery Systems & CHP*, Vol. 15, No. 7, pp. 631-640.
6. El-Genk, M. S. & Saber, H. H. (1999). Determination of operation envelopes for closed, two-phase thermosyphons. *Int. J. of Heat and Mass Transfer*, Vol. 42, pp. 889-903.
7. Joudi, K. A. & Witwit, A. M. (2000). Improvements of gravity assisted wickless heat pipe. *Energy Conversion & Management*, Vol. 41, pp. 2041-2061.
8. Park, Y. J., Kang, H. K. & Kim, C. J. (2002). Heat transfer characteristics of a TPCT to the fill charge ratio. *Int. Journal of Heat and Mass transfer*, Vol. 45, pp. 4655-4661.
9. Noie, S. H. (2005). Heat transfer characteristics of a TPCT. *Applied Thermal Engineering*, Vol. 25, pp. 495-506.
10. Negishi, K. & Sawada, T. (1983). Heat transfer performance of an ITPCT. *Int. J. Heat Mass Transfer*, Vol. 26, No. 8, pp. 1207-1213.
11. Wangnippanto, S. (1994). Study of evaporation and condensation performance in thermosyphon. M. Eng. Thesis, KMITT, Thailand, (in Thai).
12. Zuo, Z. J. & Gunnerson, F. S. (1995). Heat transfer analysis of an inclined two-phase thermosyphon. *Journal of Heat Transfer*, Vol. 117, pp. 1073-1075.

13. Terdtoon, P., Ritthidech, S. & Shiraishi, M. (1996). Effect of aspect ratio and bond number on an inclined closed two-phase thermosyphon at normal operating condition. *Proc. of the 5th Int. Heat Pipe Symposium*, Australia.
14. Booddacham, K., Tantakom, P., Terdtoon, P. & Polchai, A. (1996). Thermal behavior of a HPDE thermosyphon. *Proc. of the 5th Int. Heat Pipe Symposium*, Melbourne.
15. Payakaruk, T., Terdtoon, P. & Ritthidech, S. (2000). Correlations to predict heat transfer characteristics of an inclined closed two-phase thermosyphon at normal operating conditions. *Applied Thermal Engineering*, Vol. 20, pp. 781-790.
16. Wang, J. C. Y. & Ma, Y. (1991). Condensation heat transfer inside vertical and inclined thermosyphons. *Journal of Heat Transfer*, Vol. 113, pp. 777-780.
17. Hussein, H. M. S., Mohamad, M. A. & El-Asfouri, A. S. (2001). Theoretical analysis of laminar-film condensation heat transfer inside inclined wickless heat pipes flat-plate solar collector. *Renewable Energy*, Vol. 23, pp. 525-535.
18. Shiraishi, M., Kim, Y., Murakami, M. & Terdtoon, P. (1996). A correlation for the critical heat transfer rate in an ITPCT. *Proc. of the 5th Int. Heat Pipe Symposium*, pp. 248-254.
19. Faghri, A. (1995). *Heat Pipe Science and Technology*. Taylor and Francis Washington DC, USA.
20. Churchill, S. W. & Chu, H. H. S. (1975). Correlating equations for laminar and turbulent free convection from a vertical plate. *Int. J. Heat and Mass Transfer*, Vol. 18, No. 11, pp. 1323-1329.
21. Frank, P. & De Witt, David, P. (2002). *Introduction to heat transfer*. Incropera, 4th Edition, Chap.9.
22. Gorbis, Z. R. & Savchenkov, G. A. (1976). Low temperature TPCT investigation. *2th Int. Heat Pipe Conf.*, Bologna, Italy, pp. 37-45.
23. Huber, N. & Bowman, W. (1996). Longitudinal vibration effects on a copper/water heat pipe's capillary limits. *J. Thermophys. Heat Transfer*, Vol. 10, No. 1, pp. 90-96.
24. Abou-Ziyan, H. Z., Helali, A., Fatouh, M. & Abo El-Nasr, M. M. (2001). Performance of stationary and vibrated thermosyphon working with water and R134a. *Applied Thermal Engineering*, Vol. 21, pp. 813-830.